Stepping Statistics of Single HIV-1 Reverse Transcriptase Molecules during DNA Polymerization

Theodore P. Ortiz, Jason A. Marshall, Lauren A. Meyer, Ryan W. Davis, Jed C. Macosko, Jeremy Hatch, David J. Keller, and James A. Brozik*

Department of Chemistry, University of New Mexico, Albuquerque, New Mexico 87131

Received: April 6, 2005; In Final Form: June 24, 2005

DNA polymerases are protein machines that processively incorporate complimentary nucleotides into a growing double-stranded DNA (ds-DNA). Single-base nucleotide incorporation rates have been determined by stalling and restarting various polymerases, but intrinsic processive rates have been difficult to obtain, particularly for polymerases with low processivity, such as the human immunodeficiency virus type 1 reverse transcriptase (HIV RT) polymerase. Here we find, using a new fluorescence-based single-molecule polymerization assay, that the intrinsic processive DNA-dependent polymerization of HIV RT is approximately Poissionian (i.e. each nucleotide is added sequentially) with a rate of about 100 bases per second at 21 °C. From the same experiments, based on the stepping statistics of polymerization, we also estimate the rates for HIV RT early termination and final release of completely replicated primer−template DNA. In addition, by measuring the rate of polymerization as a function of temperature, we have estimated the activation energy for processive nucleotide incorporation.

I. Introduction

Human immunodeficiency virus reverse transcriptase (HIV RT) is a complex molecular machine that replicates the genome of the AIDS virus, first by polymerizing a DNA copy of the original RNA genome (using its reverse transcriptase activity) and then degrading the RNA strand of the resulting DNA/RNA hybrid and finally replicating the remaining DNA strand to produce a double-stranded DNA provirus. The importance of this enzyme to the life cycle of the HIV-1 retrovirus makes it a target for therapeutic drug treatments (nucleoside reverse transcriptase inhibitors, AZT, ZDV, ddC, etc., and nonnucleoside reverse transcriptase inhibitors, nevirapine, efavirenz, HEPT, etc.). As such, the rational design and development of RT inhibitors depends greatly on the extent to which the mechanisms by which the enzyme catalyzes the polymerization (reverse transcription and DNA polymerization) and depolymerization (RNase H) reactions are understood. During one cycle of polymerization (either reverse transcription or DNA replication) HIV RT, like all DNA polymerases with known structures, binds a new nucleotide and helps it pair correctly with the base that is being replicated on the template strand; closes its fingers domain, to help discriminate correct from incorrect nucleotides and to form a tight catalytic complex; catalyzes the formation of a new phosphodiester bond; reopens its fingers domain; and moves bodily to the next site along the DNA. Thus, what might be called the basic kinematics of DNA polymerase machines is known with reasonable confidence.

What is still missing is a physical understanding of how the basic parts work together, especially, what specific interactions among what specific parts give rise to function. The most important questions are centered on the energies of interaction between the various parts and on how these energies are related to structure. The overarching picture is that the protein machine moves (by diffusion) on a free energy surface, that the shape of this surface determines its mechanism and properties, and that the structure and interactions between parts give rise to this surface. The key problem then becomes to learn as much as possible (from both experiment and theory) about the free energy surface for the protein machine.[1]

Here we report results from a new kind of single-molecule kinetic measurement on the HIV reverse transcriptase. The experiment uses a fluorescently labeled nucleotide that is present in very low concentration but is necessary as a trigger to both start the stalled polymerase and label the DNA−polymerase−nucleotide complex so that it lights up when imaged through a fluorescence microscope. The complex goes dark again when the DNA is released at the end of replication, so it is possible to measure the time for replication of individual short primer−template DNAs. By plotting histograms of the replication time over many events, we are able to estimate the statistical distribution for replication time. By fitting the histograms to a simple model, we are then able to estimate the turnover rate for processive nucleotide incorporation, the rate for DNA release at the end of the template, and the rate for early release of the DNA (and photobleaching). By repeating the experiment at several temperatures, we are then able to estimate the effective Arrhenius barrier height for nucleotide incorporation, which in turn may reflect the height of the saddle point in the rate-limiting portion of the polymerase free energy surface. Together with abundant structural information on HIV RT and DNA polymerases in general,[2−4] earlier ensemble kinetics measurements,[5−16] and a recent measurement of the motor forces generated by HIV RT,[17] these results begin to establish the basic shape of the potential energy surface in the neighborhood of the rate-limiting step.

II. Materials and Methods

II.A. Sample Preparation. All experiments were performed in an aqueous buffer (10.0 mM $MgCl_2$, 40.0 mM KCl, and 25.0

* To whom correspondence should be addressed. Tel. 505 277-1658. Fax 505 277 2609. E-mail: brozik@unm.edu.

10.1021/jp051778f CCC: $30.25
Published on Web 08/02/2005

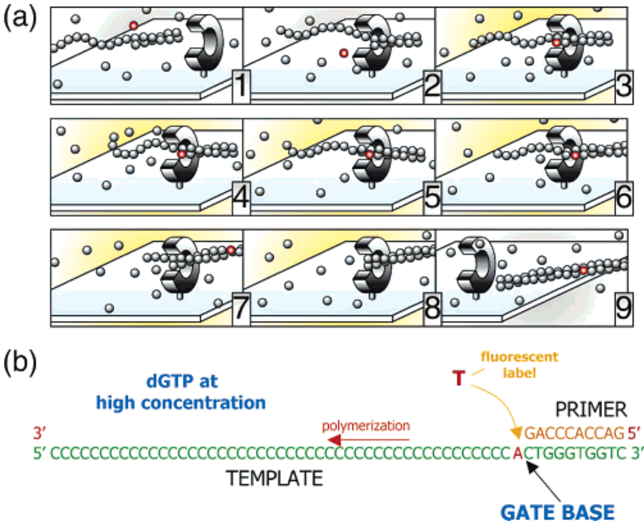

Figure 1. Experimental design. (a) Frame by frame cartoon of assay. (1) Adsorbed HIV RT on slide with DNA/DNA P/T (primer−template) and dNTPs in solution. (2) The P/T binds to active site in HIV RT. (3) Fluorescent tagged nucleotide (dUTP*) is incorporated and fluorescence is "turned on". (4) DNA advances to prepare for incorporation of the next nucleotide. (5) Second nucleotide is incorporated. (6) DNA advances to prepare for another nucleotide incorporation. (7−8) The process is repeated for *N* steps until the last nucleotide is incorporated. (9) The fully sequenced DNA strand is released and the fluorescence is "turned off". A separate background color is used in the frames to distinguish counting periods (light states) from noncounting periods (dark states). Dark states not illustrated here include the release of an incomplete DNA strand and bleaching of the fluorescent label. (b) DNA sequence used in this assay.

mM Tris·HCl, pH 7.6). Flint microscope slides (Olympus Inc.) were cleaned with concentrated sulfuric acid, rinsed thoroughly with Nanopure (18 MΩ cm) water, dried under a stream of dry N_2, and then UV-ozonated for 1 h. Reverse transcriptase (6.53 μM, Amersham Biosciences, Buckinghamshire, England) was adsorbed nonspecifically to the cleaned surface of a slide for 15 min. After removal of nonadsorbed RT by repeated rinsing with buffer, the surface of the slide was passivated with bovine serum albumen (BSA) (New England Biolabs, Beverly, MA) to prevent nonspecific binding by DNA and fluorescent nucleotides. A buffered solution (buffer described above) containing the primer−template DNA, labeled and unlabeled dNTPs, and β-mercaptoethanol (1% vol) was introduced as a hanging drop on the underside of the flint glass slide. The slide was then sealed around a chamber with silicon vacuum grease to prevent evaporation of the sample.

Primer−template DNA was formed by annealing the primer strand (5′GACCCACCAG3′), (Qiagen, Alameda, CA) to the complementary template region of the sequence (5′[C]$_n$ACTGGGTGGTC3′) (Qiagen, Alameda, CA). The template length was varied from $n = 10$ to 40 nucleotides. In each case the first nucleotide in the template sequence was a deoxyriboadenylate (dA) with the remaining residues being deoxyribocytidylate (dC). Labeled dUTP (Chromatide AlexaFluor 488-5-dUTP, Molecular Probes, Eugene, OR) was present in low concentrations (10 nM), while dGTP (Amersham Biosciences, Piscataway, NJ) was present in saturating concentrations (200 μM) based on literature estimates of Michaelis−Menton K_D and V_{max} values.[11,13−15] The sample cell was then place on top of a microscope stage.

II.B. Single Molecule Fluorescence Assay. Figure 1 depicts the single-molecule fluorescence assay. The HIV RT is nonspecifically adsorbed to a cover glass (Figure 1a), with DNA primer−template molecules and nucleotides in the surrounding solution. All the components necessary for replication (HIV RT, DNA, nucleotides, Mg^{2+}) are present, so polymerization takes place continuously as new DNAs bind to the surface-attached HIV RTs, are replicated, and then are released into solution. The template strand (Figure 1b) has a primer binding site, followed by a single A residue and then a run of C's of variable length. The nucleotides in solution include a low concentration of fluorescently labeled dUTP and a high concentration of unlabeled dGTP. As soon as a fluorescent dUTP binds, the HIV RT−DNA−nucleotide complex becomes fluorescent and lights up on the detector. It stays "on" until the polymerase incorporates enough G's to complete the template and the DNA is released, until the DNA dissociates early, or the fluorophore bleaches. The fluorescence "gate" is excited by through-objective total internal reflection (TIR) at the glass−aqueous interface (Figure 2a). The TIR illumination excites only fluorophores near the surface, which greatly reduces background fluorescence from free, unbound fluorophores. The fluorescent light is collected with a high numerical aperture microscope objective (NA = 1.67; Olympus Inc.) and fluorescence intensity is recorded as a function of time with an intensified CCD (ICCD) camera. The camera produces a full movie of events that occur in the field of view of the microscope with a frame rate set to 10 frames/s (100 ms time resolution).

II.C. Experimental Configuration. The microscope used in the single molecule fluorescence studies is shown in Figure 2a. In this apparatus, the beam from a doubled cw-Nd:YAG laser (532 nm, 10 mW, BWTEK Inc.) passes through a 532-nm laser line filter (±2 nm fwhm, OptoSigma Corp.), a calcite polarizer, and a $^1/_4$ waveplate to produce clean circularly polarized light. The beam then passes through a spatial filter, is attenuated to 1 mW with a neutral density filter, is turned 90° with a dichroic mirror (QS4SLP, Chroma Technologies Corp.), and is focused with a 500-mm focal length quartz lens onto the back focal plane of the microscope objective (Olympus Inc.) such that the deflected beam is totally internally reflected (TIR) at the flint glass/buffer interface. Fluorescence from the sample is collected through the microscope objective, passed through the dichroic mirror, filtered with a long pass filter (HQ550LP, Chroma Technologies Corp.) to remove scattered laser light, and imaged onto an intensified CCD camera (IPentaMax, Roper Scientific Inc.) with a quartz lens. Fluorescence from single molecules yields diffraction limited spots (∼250 nm) that cover a 6 × 6 area of pixels on the ICCD camera (fwhm).

For experiments involving templates of varying lengths, the temperature was maintained near 21 °C (ambient temperature), monitored with a J-type thermocouple mounted in near contact with the sample. For the temperature-dependent experiments, the temperature was changed from 21 to 30 °C in five nearly equal steps with a combination of a thermostat and a ceramic heating element. Data sets range from 15 to 20 movies of 500−1000 frames each captured with a time resolution of 100 ms per frame.

II.D. Data Analysis. Labeled dNTPs and sequenced DNA strands incorporating fluorescent tags diffuse in solution fast enough so that while they contribute modestly to the background signal, they do not appear as a definable spot at the longer signal integration times employed for these experiments. Any labeled species that have been bound either nonspecifically or as part of a sequenced DNA strand during the replication process will appear as diffraction limited spots. For each diffraction limited spot appearing in the field, the signal intensity is integrated over a 6 × 6 area for each frame of a movie, graphed as time versus

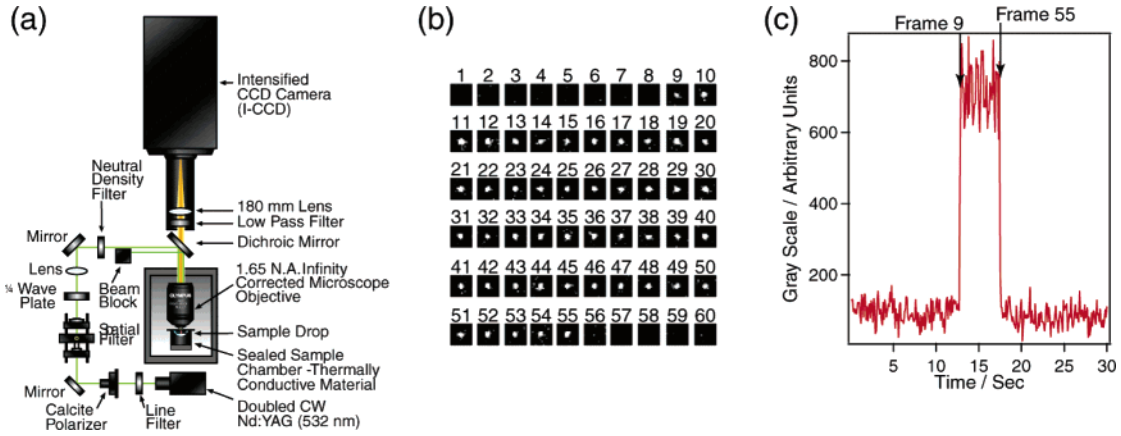

Figure 2. Fluorescence acquisition. (a) Microscope configuration; 532-nm excitation is produced by a Nd:YAG laser attenuated to ~1 mW and single molecule fluorescence is collected by a 1.4 NA infinity-corrected microscope objective imaged onto an ICCD camera operating at a 100 ms frame rate. (b) Successive frames of fluorescence images corresponding to DNA replication by an adsorbed HIV-1 reverse transcriptase. (c) Intensity data extracted from part b by integration of signal from a 6 × 6 pixel area over all frames in the movie.

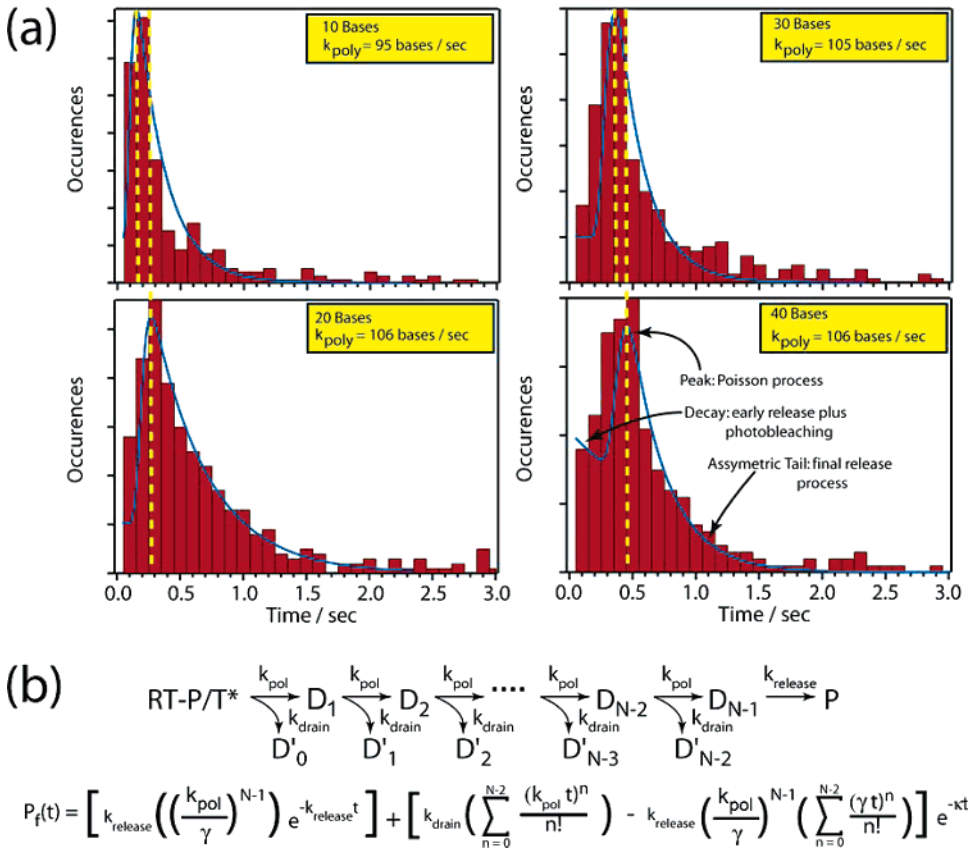

Figure 3. (a) Distribution of complete replication times for HIV RT carrying out DNA-dependent DNA polymerization. Poly-C templates of length 10, 20, 30, and 40 bases long with 200 μM dGTP at 21 °C. Solid blue lines are least-squares fits to the kinetic model described in part b. Vertical dashed yellow lines indicates the most probable intrinsic processive polymerization times for each template length. (b) Model and corresponding time distribution. $P_f(t)$ is the experimentally observed distribution (or histogram) of fluorescence "on" times, N is the length of the template, k_{pol} is the transition rate for intrinsic processive nucleotide incorporation, k_{drain} is the combined loss-of-fluorescence transition rate, $k_{release}$ is the end-of-template DNA release rate. Intermediate states (D_1−D_{N-1}) are HIV RT-DNA complexes for primer lengths extended by n bases. Drain states (D'_0−D'_{N-2}) and the product (P) are dark states (either because the DNA has been released or the fluorophore has bleached) for which no fluorescence is observed.

intensity, and recorded. Replication times are measured as the length of time a diffraction limited spot stays on (see Figure 2b,c). A histogram is then constructed from the recorded values and the data are fit (IGOR Pro 3.13) to the kinetic equation given in Figure 3b. A detailed explanation and derivation of this equation is presented in the Supporting Information.

III. Results

III.A. Rates for Processive Polymerization, Early Termination, and ds-DNA Release. Figure 2b shows a series of frames with a bright spot corresponding to a single active HIV RT, and Figure 2c shows the corresponding intensity vs time trace for one HIV RT replicating one DNA template.

Figure 3a shows histograms of fluorescence "on" times collected from many such movies, for template lengths of 10, 20, 30, and 40. Because replication is a stochastic process, each replication run takes a different length of time to complete, and the histogram represents a measurement of the probability distribution for the replication time.

The replication time distribution can be modeled by a stochastic process with three types of transitions: intrinsic processive nucleotide incorporation, early loss-of-fluorescence (combined early DNA dissociation and photobleaching), and release of DNA after complete replication of the template. The model and the expression for the time distribution is shown in Figure 3b, where $P_f(t)$ is the experimentally observed distribution (or histogram) of fluorescence "on" times, N is the length of the template, k_{pol} is the transition rate for intrinsic processive nucleotide incorporation, k_{drain} is the combined loss-of-fluorescence transition rate, $k_{release}$ is the end-of-template DNA release rate, $\kappa = k_{pol} + k_{drain}$, $\kappa_R = k_{release} + k_{drain}$, and $\gamma = \kappa - k_{release}$.

Though this (mathematically exact) expression is rather opaque, the main features of the distribution are easily interpreted, as shown in Figure 3a. The curve can be qualitatively described as a sum of a Poisson peak (representing the processive polymerization process), an exponential (representing the combined early-loss-of-fluorescence processes), and a long asymmetric tail (representing the effects of the DNA release process at the end of the template). To a first approximation, the maximum of the peak gives k_{pol}, the shape of the tail gives k_{rel}, and the exponential gives k_{drain}. It is worth noting that the value of k_{pol} measured in these experiments is for *processive* polymerization (one nucleotide after another), and so is somewhat different and complementary to the value measured in ensemble pre-steady-state experiments, which is the measured rate for incorporating the first base after a stall.[5,6]

In the actual analysis of the histograms, the parameters k_{pol}, k_{drain}, and $k_{release}$ were allowed to vary to achieve the best fit. The early termination and bleaching rate, k_{drain}, is ~2 orders of magnitude slower than the processive polymerization rate, k_{pol}, so once replication has started, it goes to completion in the great majority of cases, at least for templates up to 40 bases in length. The average rates obtained from the whole set of varying template oligomers are $k_{pol} = 103 \pm 5\ s^{-1}$, $k_{drain} = 0.6 \pm 0.3\ s^{-1}$, and $k_{release} = 3.7 \pm 0.7\ s^{-1}$. The ratio $k_{pol}/k_{drain} \cong 172$ is a lower bound on the processivity of HIV RT for this template, temperature, and buffer.

The fact that a simple Poisson distribution fits the peaks of the histograms is consistent with a turnover cycle with one rate-limiting step, in agreement with earlier results from ensemble pre-steady-state kinetics and recent single molecule studies on the mechanical properties of HIV RT.[17] It also shows that there is little heterogeneity from one HIV RT to the next. This is important, since it is evidence that adsorption of HIV RT to the surface is not a big perturbation.

As expected, there is a clear increase in overall replication times as the template oligonucleotide length increases. This is a convincing verification of the experimental design, and the maxima (from fit of the data) in Figure 3a define the most probable replication time (t^*) for each template length. A plot of t^* vs template length is linear with a slope of 0.01 s ($k_{pol} = 100\ s^{-1}$) and an intercept of 0.05 s ($k_{release} = 20\ s^{-1}$), in general agreement with our other estimates. The fact that the plot is linear helps rule out significant interference by the fluorescent label, because the label would affect the short DNA template lengths more than the long ones. For a 10-base template, the label never clears the protein, for example, while for a 40-base template the label has cleared the protein after at most 20 bases pass. If the label had a significant effect on the rate, the 40-mer would show a different (probably faster) mean rate per base than a 10-mer. The plot in Figure 4a shows that this is not the case.

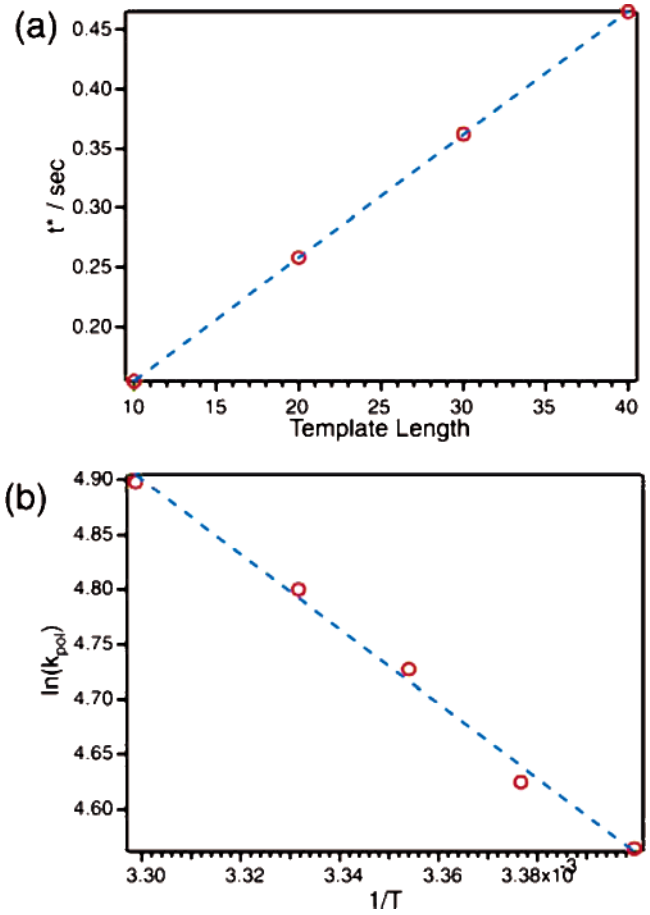

Figure 4. (a) Plot of most probable replication time vs DNA template length. Circles are experimental data and the dashed line is a linear fit. The slope gives $k_{pol}^{estimate} = 100\ s^{-1}$ and the intercept gives $k_{release}^{estimate} = 20\ s^{-1}$. (b) Arrhenius plot of $\ln(k_{pol})$ vs $1/T$. Circles are experimentally derived k_{pol} values from best fits of histograms to the kinetic model depicted in Figure 3b.

III.B. The Activation Energy for Processive Polymerization. HIV RT is quite sensitive to changes in temperature, as shown in Figure 4b, where the logarithm of the rate constant is plotted vs inverse temperature (Arrhenius plot). These data were collected for templates of length 40, at saturating dGTP concentration, between a low temperature of 21 °C and an upper temperature of 30 °C. Despite the narrow temperature range, the rate of polymerization changes by a factor of 1.4. With the slow time resolution of the ICCD camera, it was not possible to measure the intrinsic processive polymerization rate at 37 °C directly, but extrapolation of the line in Figure 4b yields a rate ~174 bases/s. The activation barrier, found from the slope of $\ln(k_{pol})$ vs $1/T$, is estimated at about 28 kJ/mol.

IV. Discussion

Single-molecule fluorescence experiments have several intrinsic advantages over ensemble methods: (1) Concentrations of protein and DNA are irrelevant: populations are generated directly by counting. (2) Inactive protein, incomplete complexes, etc. are less important sources of error; most are invisible and hence do not contribute. (3) It is not necessary to synchronize

the starting state of an ensemble of many molecules. (4) A full statistical distribution of times is generated instead of an ensemble average. In addition, the relatively simple single molecule experiment outlined above is quite readily adapted to new systems or new experiments, e.g, investigating the effects of sequence, mutants, primers, RNA templates, or inhibitors.

Pre-steady-state kinetic studies using quench flow techniques have reported k_{pol} rates for the incorporation of the first few nucleotides ranging from less than 10 bases per second up to ~100 bases per second at 37 °C.[5−16] In these studies the protein-DNA complex is preformed and then triggered by the addition of either nucleotides or Mg^{2+}. (The measured rates in these studies are not affected by the binding and unbinding of the DNA to the enzyme, which is a much slower process then the fingers-closing step and greatly reduces the observed effective polymerization rates measured in simpler steady-state kinetic studies.[6,11,12]) The experiment reported here measures the best-fit intrinsic processive incorporation rate over the entire template, as opposed to the rate of incorporation of the first base after a stall. The rate we find, about 100 bp/s at 21 °C and an estimated 170 bp/s at 37 °C, is considerably faster than those reported for pre-steady-state experiments. Most of the potential difficulties in the single molecule experiment—interference from the fluorescent label or from adsorption of HIV RT to a substrate—are expected to reduce the polymerization rate rather than increased it. We therefore attribute the difference to buffer conditions, template sequence, the first base rate vs processive rate difference, and possibly the presence of inactive or partially active HIV RT in some ensemble experiments.

All complex molecular machines such as HIV RT can be understood as mechanochemical devices, constructed of several molecular parts (DNA, protein subdomains, nucleotides, etc), each with its own characteristic motions and properties. The interactions of these parts with each other and with substrates and products determine the mechanism and capabilities of the protein machine. As mentioned earlier, interactions among the parts give rise to a free energy surface, and the operation of the machine is then a process of diffusion in the conformational state space of the machine, guided by the contours of this free energy surface. Moreover, a potential energy surface (or series of potential energy surfaces) can be used to understand and predict how the machine will respond to changes in environment (temperature, substrate chemical potential, etc.) and external forces. Information about a machine's free energy surface is therefore a potentially very powerful way of reaching a well-founded understanding of the machine.

It is not difficult to estimate the main features of the free energy surface from structure and basic kinetics.[18] The main conformational changes are the movements of the fingers, the movement of the protein along the DNA, the alignment and stacking of the template base in the active site, and the binding of nucleotide. The variables that describe these changes define the state space of the system. The scale of the motion for each variable, and hence the basic shape of the free energy surface, is determined by the structure of the protein−DNA−nucleotide complex. What remains beyond these basic features are the quantitative aspects, mainly the depths of potential energy wells and barriers. Earlier results from pre-steady-state kinetic experiments indicate that the closing of the fingers domain is the rate-limiting step in the overall turnover cycle,[19,20] and the rate of fingers closing is essentially equivalent to the overall rate of polymerization, k_{pol}. The activation barrier reported here can be interpreted as an estimate of the energy barrier that must be surmounted to deform the fingers domain from its open to its closed conformation. This taken together with an earlier estimate of the barrier width from force pulling experiments [17] begin to define at least one key region (the fingers closing step) of the potential energy surface for HIV RT.

Acknowledgment. This work was supported by National Institutes of Health Grant GM63808 (to J.A.B and D.J.K.). Graduate student support (to T.P.O and R.W.D.) was provided by the Cross-disciplinary Optics Research and Education (CORE) program, an Integrative Graduate Education and Research Training (IGERT) project funded by the National Science Foundation.

Supporting Information Available: Detailed explanation of the full derivation of the kinetic equations developed on the basis of the proposed mechanism for the polymerization of fluorescently tagged oligomer with a template composed of two nucleotide types with identical rate constants. This material is available free of charge via the Internet at http://pubs.acs.org.

References and Notes

(1) Keller, D. J.; Bustamante, C. *Biophys. J.* **2000**, *78*, 541.
(2) Ding, J. P.; Das, K.; Hsiou, Y.; Sarafianos, S. G.; Clark, A. D.; JacoboMolina, A.; Tantillo, C.; Hughes, S. H.; Arnold, E. *J. Mol. Biol.* **1998**, *284*, 1095.
(3) Kohlstaedt, L. A.; Wang, J.; Friedman, J. M.; Rice, P. A.; Steitz, T. A. *Science* **1992**, *256*, 1783.
(4) Huang, H.; Chopra, R.; Verdine, G. L.; Harrison, S. C. *Science* **1998**, *282*, 1669.
(5) Pop, M. P.; Biebricher, C. K. *Biochemistry* **1996**, *35*, 5054.
(6) Wöhrl, B. M.; Krebs, R.; Goody, R. S.; Restle, T. *J. Mol. Biol.* **1999**, *292*, 333.
(7) Huber, H. E.; McCoy, J. M.; Seehra, J. S.; Richardson, C. C. *J. Biol. Chem.* **1989**, *264*, 4669.
(8) Majumdar, C.; Abbots, J.; Broder, S.; Wilson, S. H. *J. Biol. Chem.* **1988**, *263*, 15657.
(9) Hseih, J.-C. S. Z.; Modrich, P. *J. Biol. Chem.* **1993**, *268*, 24607.
(10) Furge, L. L.; Guengerich, F. P. *Biochemistry* **1999**, *38*, 4818.
(11) Krebs, R.; Immendorfer, U.; Thrall, S. H.; Wöhrl, B. M.; Goody, R. S. *Biochemistry* **1997**, *36*, 10292.
(12) Kerr, S. G.; Anderson, K. S. *Biochemistry* **1997**, *36*, 14064.
(13) Zinnen, S.; Hsieh, J.-C.; Modrich, P. *J. Biol. Chem.* **1994**, *269*, 24195.
(14) Spence, R. A.; Anderson, K. S.; Johnson, K. A. *Biochemistry* **1996**, *35*, 1054.
(15) Wöhrl, B. M.; Krebs, R.; Thrall, S. H.; Le Grice, S. F.; Scheidig, A. J.; Goody, R. S. *J. Biol. Chem.* **1997**, *272*, 17581.
(16) Cramer, J.; Strerath, M.; Marx, A.; Restle, T. *J. Biol. Chem.* **2002**, *277*, 43593.
(17) Lu, H.; Macosko, J.; Habel-Rodriguez, D.; Keller, R. W.; Brozik, J. A.; Keller, D. J. *J. Biol. Chem.* **2004**, *279*, 54529.
(18) Keller, D. J.; Brozik, J. A. *Biochemistry* **2005**, in press.
(19) Rothwell, P. J.; Berger, S.; Kensch, O.; Felekyan, S.; Antonik, M.; Wöhrl, B. M.; Restle, T.; Goody, R. S.; Seidel, C. A. M. *Proc. Natl. Acad. Sci. U.S.A.* **2003**, *100*, 1655.
(20) Deval, J.; White, K. L.; Miller, M. D.; Parkin, N. T.; Courcambeck, J.; Halfon, P.; Selmi, B.; Boretto, J. l.; Canard, B. *J. Biol. Chem.* **2004**, *279*, 509.